MEASUREMENTS OF LOCAL VELOCITIES INSIDE THIN LIQUID FILMS IN HORIZONTAL TWO-PHASE FLOW

S. V. Paras and A. J. Karabelas
Department of Chemical Engineering and
Chemical Process Engineering Research Institute
University Box 455, GR 540 06 Thessaloniki, Greece

ABSTRACT

A new experimental facility based on Laser Doppler Anemometry permits accurate local measurements in a horizontal pipe. Measurements of the axial velocity component in the liquid layer of the atomization/ stratified flow regime are reported. The new information includes time averaged local velocities, RMS values, probability density distributions, and power spectra. Elimination of velocity bias and calculation of velocity spectra is accomplished by a recently developed "signal reconstruction" algorithm.

The data suggest that only in the vicinity of the solid surface (sublayer) does the liquid motion resemble the well-known behavior of single phase flow. Beyond that, the flow field is strongly influenced by the wavy gas/liquid interface and by the apparently intensive energy transfer from the very fast moving gas to the liquid layer.

Keywords: gas-liquid flow, local velocity, thin film, LDA.

Presented in the 26th Meeting of
'The European Two-Phase Flow Group',
Hosted by ENEA, Rome, 27-29 May 1991.

1. INTRODUCTION

In horizontal gas-liquid pipe flow, relatively thin liquid layers (of order 1 to 10 mm thick) are dominant elements of some flow patterns at relatively small liquid rates. Typical cases of this type are the "annular" and "atomization" flow regimes prevailing at high and intermediate gas rates, respectively (Figure 1). The common characteristic of these flow regimes is the ***wavy liquid layer***, flowing at the pipe ***bottom*** under the influence of the much faster moving gas. In annular flow, as is well known, the rest of the pipe circumference is also covered by a continuous thin liquid film, whereas in the atomization regime stagnant droplets or rivulets are observed in the upper part of the pipe wall.

The work reported here is part of an effort to gain information, through local velocity measurements, on the flow structure inside thin liquid layers in horizontal pipe flow. To the best of the authors knowledge, no data of this type are available in the literature. Well developed experimental techniques, such as hot wire or hot film anemometry, cannot be used in this case due to the unavoidable probe interference with the flow.

Non-intrusive optical techniques, such as Laser Doppler Anemometry (LDA), are obviously a promising approach. However, the complexity of the 3-D flow field and some inherent problems (to be outlined in subsequent sections) have apparently prevented researchers from obtaining the much needed information on the flow field within liquid layers. Data of some relevance to this study are presented by Strumolo et al. (1985) and Fabre et al. (1983). In the former, some LDA measurements are reported for a vertical falling film, but very limited information is given about the experimental techniques. In the latter, LDA data are included, taken in a relatively ***deep*** liquid layer of stratified air/water flow through a channel of rectangular cross-section.

The lack or relevant velocity data has some inevitable consequences. For example, all recent efforts to model liquid layers in horizontal two phase flow (e.g. Shoham & Taitel, 1984; Laurinat et al., 1985; Andritsos & Hanratty, 1987; Fukano & Ousaka, 1989) are based on well-known expressions for ***single*** phase flow, ignoring the effect of the wavy gas/liquid interface. Yet detailed film thickness measurements (e.g. Laurinat, 1982 and Paras & Karabelas, 1991) show quite large intensities (RMS over mean values) of film thickness fluctuations. Moreover, the very recent flow visualization study carried out by Jayanti & Hewitt (1990) in horizontal annular flow, suggests that the influence of these fluctuations on the velocity distribution within the film is quite significant.

This paper describes first the experimental set-up, designed with the main requirement to permit LDA measurements within liquid films in horizontal pipe flow. The LDA system is based on a single beam Argon-ion laser. Bias of the raw velocity data is eliminated by using a new signal "reconstruction" method (Veynante & Candel, 1988), which is briefly outlined. Axial velocity measurements are reported next, obtained mainly in the atomization regime. Local mean velocities, RMS values, probability density distributions and power spectra (PSD) are computed from the "reconstructed" signals.

2. VELOCITY MEASUREMENTS IN THIN LIQUID LAYERS

2.1. Flow loop

The velocity measurements are carried out in a horizontal flow loop described in some detail elsewhere (Paras & Karabelas, 1991). Two-phase flow develops in a 50.8 mm i.d. pipe loop with a 16 m long straight section. Experiments are made in a glass test section positioned about 300 diameters downstream of the mixing section of the two phases, where the flow is considered to be fully developed.

Water is circulated in the loop after it is passed through a system of water filters (0.5 μm final pore size). The water flow rate is measured using a bank of 3 rotameters, each covering part of the range of flow rates (max. 0.4, 1.2, 2.6 m^3/hr). The accuracy of the rotameters is better than ± 1%. Air is supplied by two compressors with a total capacity of 15 m^3/min (at 1 atm) and its flow rate is measured by an orifice plate with an accuracy of ± 5%.

2.2. Experimental technique

The LDA set-up described here was developed during the course of this work in order to make measurements of local velocities within a liquid film layer near the pipe wall in horizontal two-phase flow. Figure 2 shows the general arrangement of the LDA system, which operates in the fringe mode. The green beam from a 5W Argon-Ion laser source, having a wavelength of 514.5 nm and a maximum power of 2 W, is split into two identical beams by an optical arrangement supplied by DANTEC. The central beam is fed through a Bragg cell and is optically shifted by 40 MHz. The two beams are focused, using a 80 mm focal-length lens. The intersecting beams form an ellipsoidal measuring volume with major and minor axes (in air) 91 μm and 23 μm, respectively . The

angle of intersection is Θ=28.1° and the optical fringe pattern formed in this measuring volume has a spacing (δ) of 1.06 µm [calibration factor= 1.06 (m/s)/MHz]. Back-scattered light is collected onto a photomultiplier through the same lens.

The optical properties or the media (air, water, glass), through which the laser beams are passing, require special attention since refraction at interfaces changes the paths of the laser beams thus displacing their point of intersection and modifying the angle between the beams. In particular, the effect of the water on the probe volume characteristics must be taken into account. The diameter of the measuring volume (dx), the fringe spacing and the number of fringes are unaffected by the presence of the water. On the other hand the length of the probe (dz) and its position from the wall are somewhat increased as compared with air (Ross, 1984). Within the flow field (in water) the wave-length and the beam intersection angle is reduced to 386.8 nm and 21°, respectively, whereas the major axis of the measuring volume dz is increased to 121 µm (Table 1). The point of intersection of the beams in water is displaced by Δy for a translation Δx of the optical system in air. It can be proven (Ross, 1984) that $\Delta y = n_W \cdot \Delta x$, where n_W is the refractive index of the water.

Table 1. Parameter values of the LDA system.

parameter	λ nm	f mm	D mm	Θ deg	dx µm	dy µm	dz µm	δ µm
in air	514.5	80.0	40	28.1	23	22	91	1.06
in water	386.8	106.4	40	21.0	23	22	121	1.06

Particles passing through the measuring volume produce a scattered light signal whose frequency (f_D) is related to particle velocity (V) by

$$V = \frac{f_D \lambda}{2\sin(\Theta/2)}$$

where λ is the laser light frequency and Θ is the beam intersection angle. The resulting photomultiplier output signal is fed to a Counter Signal Processor (DANTEC 55190) which measures the time taken by a particle to traverse a specified number of fringes (i.e. 8 fringes) of the measuring volume. The basic system described above cannot discriminate between positive and negative velocities. For this reason a frequency shift (DANTEC 55N10) is applied to one of the beams.

A special support unit for the LDA system was constructed in our laboratory in order to allow precise spatial movement (x, y, Θ) of the measuring volume (Figure 3). The entire optical system [1] is fixed onto an adjustable "arm" [2], in a direction perpendicular to the main pipe axis [3]. The use of a balancing weight [4] permits the effortless rotation of the LDA optics by 360° around the pipe axis in step intervals of one degree. A tightening mechanism [5] secures the required position. In addition to this rotary motion, two precise x-y micrometers [6] (Spindler & Hoyer GMBH Co.) with 8 cm maximum translation and 10 μm resolution provide the fine horizontal and vertical adjustments. For the gross vertical movements long bolts [7] on the main support unit are used. To further ensure that the optical system center of rotation coincides with the axis of the pipe, a concentric adjustment ring surrounds the pipe [8]. In this manner, the LDA measuring volume can be located with precision at any point within the pipe cross-section. Vibration absorbing pads [9] ensure the vibration-free operation of the whole system.

The test section is a 50.8 mm i.d. pipe with a uniform wall thickness (t=3.81 mm ± 25 μm) made of high precision glass (Pyrex #7740) which has a constant refractive index (n_{gl}=1.474)

In conventional LDA systems the laser source is fixed behind the optical arrangement and its axis coincides with the optical axis of the entire system. With this setup it is impossible to rotate the optical system with the laser source around the pipe axis. In order to overcome this problem, a flexible 5 m long optical link connects the laser source with the rest of the system permitting the beam transmission from the source to the rotatable optical system. The fiber optic link consists of input coupling optics, a single-mode polarization stable optical fiber and collimating output optics. The fiber has a 5 μm core diameter, a 125 μm cladding diameter and a 50% coupling efficiency.

With LDA one measures the velocity of scattering particles carried by the fluid. Therefore, the scattering particles must satisfy some criteria (Drain, 1986):

a. They must follow the flow (small particles).
b. Their diameter must be of the order of the fringe spacing (≈0.59 δ).
c. Their concentration must be optimum in order to improve the quality of the signal (signal to noise ratio, SNR) and the rate of the valid measurements.

In the tests carefully filtered water is seeded with monodisperse polystyrene spheres having a mean diameter 0.6 μm.

Several trials were carried out to test the operation of various parts of the LDA system. Before attempting any measurements, the LDA was aligned as accurately as possible by eye so the intersection of the beams was coincident

with their waists. The probe was then focused onto a rotating disk which was rotated with known angular velocity. The experiments showed a very good agreement between expected and measured velocity (better than 1%).

2.3. Description of the experiments

Most of the axial velocity measurements reported here were obtained in the so-called ***atomization*** flow regime. As shown in Figure 1, the latter is an intermediate regime, displaying the basic features of wavy stratified flow (liquid layer at the pipe bottom) with droplets entrained by the gas as in the annular regime. The atomization regime appears to be relatively simple for making measurements which would be also helpful in better understanding horizontal annular two-phase flow.

Velocity data were obtained for four different flow conditions corresponding to wavy stratified and atomization flow regimes. The superficial gas velocity was kept constant (i.e. U_G=11.9 m/s) and the superficial liquid velocity varied from 2.4 to 10.2 cm/s (Table 2). Axial velocity profiles were measured mainly at two circumferential locations around the pipe, i.e. at $\Theta=0^o$ (pipe bottom) and $\Theta=20^o$ (Figure 1). Additional measurements at $\Theta=10^o$ were carried out only for RUN A. The measuring system was designed to permit accurate measurements at distances as close as 100 μm from the pipe wall, which corresponds to a y^+ in the range of 4 to 6.

There is always the possibility of obtaining erroneous results by trying to measure close to an air/water interface. Laser light coming from ***reflections*** at the interface acts as a spurious "reference beam" reaching the photomultiplier. The resulting signals may be interpreted as differential Doppler signals, leading to entirely wrong results (Drain, 1986). For this reason measurements are made 1-2 mm far from the interface to avoid reflections. For the same reason, reliable measurements in very thin liquid films, in annular flow, are impossible using the previously described test section.

Only the axial component of the velocity was measured. The normal component of the velocity was impossible to measure accurately with this test section; the pipe wall acts as a convex lens, due to its curvature, thus increasing the angle of intersection of the beams and moving the real position of the intersection closer to the optical system.

The mean data rate was 100 to 200 Hz, depending on the local mean velocity. This sampling frequency was sufficient to permit frequency discrimination up to 50-100 Hz. The sample size for each run was 8000 points.

2.4. Data acquisition and statistical analysis

Signals are accepted into a buffer interface and fed to a computer (IBM-XT 286) via an IEEE-488 interface for storage and statistical analysis. For every valid measurement, the Counter transmits to the buffer interface (1kb) the Doppler frequency and the time between two successive measurements. A fast computer and the appropriate software provide measurements with high acquisition rate (maximum rate 5 kHz).

One of the basic problems in LDA is the discontinuity of the signal and the random time intervals between recorded data points, because a data point is collected *only* when a particle passes through the measuring volume. For uniformly seeded turbulent flows, during periods of relatively high velocity more particles are measured than during periods of relatively low velocities. As is well known, these characteristics can cause serious errors ("bias") in the calculation of various statistical quantities as well as practical problems in computing power spectral densities (PSD) and autocorrelation functions of the fluctuating velocity. If the sample mean velocity is calculated by simply summing up the velocities of all the measured particles and dividing by the number of particles, this arithmetic mean is higher than the true time-averaged liquid velocity (McLaughlin & Tiederman, 1973; Adams et al., 1984).

Buchhave & George (1979) propose weighting each measurement by the particle residence time in the measuring volume or by a factor inversely proportional to the measured component of the velocity at this point (McLaughlin & Tiederman, 1973). Weighting by the interarrival time between two successive particles is another method to avoid velocity "bias" (Adams et al., 1984).

Alternatively, Adams et al. (1984) suggest that the digital Counter signal could be turned into an "analog-like" signal with a Digital-to-Analog Converter and subsequent resampling with an A/D. Obviously, the successive conversions of the original signal reduce its quality.

Veynante & Candel (1988) suggest a signal reconstruction method which is time consuming but gives results almost identical with the true values. This method uses an extension of Shannon's theorem derived by Clark, Palmer & Lawrence (1985). The reconstructed signal is then resampled and the resulting sequence is analysed with standard methods. The method is restricted to situations in which the mean sampling frequency is greater than the highest frequency expected in the flow.

New software to solve the above problems was successfully developed and tested. This software is based on the above technique permitting ***reconstruction*** of an unequally spaced signal to overcome this peculiarity of the LDA signal. It performs a statistical analysis of the reconstructed signal (computation of mean, RMS, moments of high order, probability density function), Fast Fourier Transform (FFT), autocorrelation, as well as the necessary graphical representations.

3. RESULTS

Experimental conditions and some flow parameters are summarized in Table 2. U_L and U_G are the superficial liquid and gas velocities, respectively. Time records of the liquid film thickness at the pipe bottom, h, are obtained with a conductivity probe technique (Paras & Karabelas, 1991). Its mean value, h_o, is found to be in close agreement with model predictions (Andritsos & Hanratty, 1987). The RMS values of film thickness fluctuations at the bottom are larger in the case of high liquid flow rates (run A). These relatively higher RMS values are indicative of the larger disturbance waves, traveling at the interface, which are associated with higher rates of liquid atomization. In visual observations made during the runs, this behavior was clearly evident; the highest atomization rates were observed in run A and no atomization took place in run D (lowest RMS value).

The parameter U_{LF} represents the real mean liquid velocity computed on the basis of the cross-sectional area covered by the liquid, which is obtained from the measured film thickness; R_h is the hydraulic radius and $Re_{LF} = \frac{4 R_h U_{LF}}{\nu}$ the liquid film Reynolds number.

Table 2. Experimental conditions and summary of results.

run	U_L cm/s	U_G m/s	h_o mm	RMS mm	U^* (1) m/s	U at y=100μ	U^* (2) m/s	U_{LF} m/s	R_h mm	Re_{LF}
A	10.2	11.9	**7.6**	1.04	**0.069**	0.450	0.067	1.09	2.48	8802
B	7.6	11.9	**6.5**	0.88	**0.066**	0.440	0.066	1.02	2.13	7054
C	4.0	11.9	**4.4**	0.70	**0.058**	0.344	0.059	0.95	1.45	4470
D	2.4	11.9	**3.4**	0.61	**0.054**	0.297	0.055	0.83	1.12	3033

(1) Prediction (2) Equation 2

3.1. Axial velocity distributions

Figure 4 shows a typical signal of the axial velocity before and after the previously outlined "reconstruction" process. Comparison between the biased quantities and those obtained from the reconstructed signal shows that ***direct*** statistical calculations (from the raw data) of the time averaged local velocity and its RMS (u') value are higher by 5-10% and 15-20%, respectively. In Figure 5 a comparison is made of the axial velocity (U) profiles and the u' profiles, at $\Theta=0^o$ for run A, between the "original" and the "reconstructed" data sets.

The axial velocity distributions for run A and for three different circumferential positions, i.e. 0°, 10° and 20°, are presented in Figure 6. An inflection point is observed at a distance from the wall close to y=1.5 mm (y^+=60). Up to this distance, there is no appreciable difference between measurements at the three different angles, whereas farther from the wall the time averaged velocity tends to decrease with increasing of the angle Θ.

The velocity data can be normalized with respect to a friction velocity at the wall, U^*, calculated by the method proposed by Andritsos & Hanratty (1987). Values of U^* calculated from data very close to the wall (y=100 μm, y^+=4 to 6 for these experiments) are in good agreement with those obtained from the Andritsos & Hanratty model predictions as shown in Table 2. In these calculations it is assumed that there is a turbulent sublayer so that

$$u^+ = y^+ \qquad (1)$$

and

$$U^* = \sqrt{\frac{\nu\, U|_{y=100}}{y}} \qquad (2)$$

This assumption is justified on the basis of data presented in the following section. Figure 7 presents the profiles of the normalized velocities obtained at $\Theta=0^o$ and $\Theta=20^o$. The solid line represents the well-known time-averaged turbulent velocity profile for single phase flow (Schlichting, 1960). A systematic deviation from the single phase profile is observed, which is larger for the thinner layers (runs C and D). Strumolo et al. (1985) report similar results for velocity measurements inside falling films which are covered by waves.

The time averaged axial velocity profile is apparently influenced by the presence of large waves at the gas/liquid interface. Evidence supporting this

argument is provided by the fact that the velocity measurements generally differ between positions equidistant from the wall but at a different distance from the interface, as shown in Figure 6.

3.2. Turbulence intensity

Ueda & Hinze (1975) and Kreplin & Eckelmann (1979) found that in fully developed turbulent flow the axial velocity fluctuations normalized with the friction velocity U^* exhibit a maximum value between 2.8 and 3 at a distance $y^+ \approx 13$ over a wide range of Reynolds numbers (5000-82000). Figure 8 shows that there is good quantitative agreement between the above result and the data of this work, in the wall region ($y^+<30$). The profiles in this figure correspond to $\Theta=0^o$ (pipe bottom). The influence of the wavy interface appears to extend deeper into the wall region with decreasing film thickness. This observation is made by comparing the data (Figure 8) with the profiles measured by Ueda & Hinze (1975) and Kreplin & Eckelmann (1979). Indeed, the latter tend to be in better agreement with the data corresponding to the thicker films (run A). Finally, it is pointed out that the high level of the normalized velocity fluctuations, u'/U^*, away from the wall ($y^+>30$) is obviously associated with waves at the interface and/or with gas-liquid interfacial shearing.

Measurements at $\Theta=20^o$ for the thin layers of runs C and D, show a maximum at the same y^+, but the ratio u'/U^* is almost twice that measured at $\Theta=0^o$ (Figure 9). This behavior is also attributed to the influence of the interfacial waves on the velocity fluctuations, which are intensive throughout the thickness of the liquid layer.

Measurements of the axial velocity fluctuations (u') normalized with the time averaged velocity U are presented in Figure 10. The data for $y^+<30$ appear to exhibit the same behavior as in measurements in single phase flow (Ueda & Hinze, 1975). Beyond this location ($y^+>30$), the intensity is larger than that observed in single phase turbulent flow, for reasons outlined above.

3.3. Probability density distribution-Power spectra

The Probability Density functions of velocity fluctuations are Gaussian at points near the wall (Figure 11). However, two kinds of distributions are distinguished near the interface. For run A (large waves at the interface) the modal value is in the range of negative u' values, i.e. in low values of velocity (Figure 11a). On the other hand for run D, where small waves and no atomization are observed, the modal value is in the range of positive u' values

related to high values of velocity (Figure 11b). This effect is in agreement with recent observations made by Hewitt et al. (1990). These authors using a flow visualization technique observed the instantaneous axial velocity profiles in the liquid film in horizontal annular air/water flow. They reported two types of velocity profiles: the distorted S-shaped profile prevailing in film flows subjected to interfacial shear ***without waves***, and the parabolic type occurring during the passage of a wave.

To summarize, it appears that near the interface the axial velocity may have relatively large values, when no large waves are present (run D), or low values associated with the passage of large disturbance waves (runs A & B). In the substrate the behavior is the same as in single phase turbulent flow.

The calculated velocity spectra reinforce the observation that there is a significant influence of the large waves on the liquid film flow. Figure 12a shows the power spectral density (PSD) for two points (run A), at y=5 mm (close to the interface) and y=0.1 mm (close to the pipe wall). Figure 12b shows the PSD for run D, for y=2 mm and y=0.1 mm. Most likely the characteristic modal values of the spectra correspond to the frequencies of the large waves in stratified flow (1-10 Hz) reported by Andritsos (1986).

Figures 13a and 13b show that in logarithmic coordinates the slope of the PSD curves in the high frequency range is roughly -5/3. This result is additional evidence that the flow within the thin liquid films is ***turbulent***.

4. CONCLUDING REMARKS

The data, especially the distribution of intensities and the power spectra, show that the flow field in the relatively thin liquid layers examined here is turbulent. The distribution of intensities is the same as that for single phase flow only close to the wall ($y^+<30$).

A significant result obtained from the data (Figure 7) is the relatively low time-averaged axial velocity, U^+, far from the wall ($y^+>10$), as compared with the velocity profile for single phase flow. However, in this part of the flow field, the measured intensity of velocity fluctuations (Figures 8, 9, 10) is generally higher than that prevailing in single phase pipe flow. In fact, the intensity, u'/U^*, tends to increase as the gas/liquid interface is approached (Figure 9).

The existence of strong normal velocity components (along a plane vertical with respect to the main flow direction) could be an explanation for the above behavior. Furthermore, it is possible that the kinetic energy transfer from the faster moving gas to the liquid, through the interface, leads to the formation

of coherent structure, (i.e. vortices) characterized by significant normal and reduced axial velocity components.

To the best of the authors knowledge, there are no other measurements, for the same geometry and flow conditions, available for comparison. However, the measurements reported here are in qualitative agreement with similar data obtained by Fabre et al. (1983) for stratified air/water flow in a horizontal channel of rectangular cross-section. The liquid layers in that case were considerably thicker compared with those of the present study. Their measurements show significant values of the normal velocity component, and reduced time-averaged axial components near the air/water interface.

The characteristic frequencies in the power spectra seem to correspond to the frequencies of the large disturbance waves. The probability distribution when these interface waves are large (run A, Figure 11a), combined with the evidence on axial velocity distribution, suggest that the previously described coherent structures (vortices) are very likely an essential element of the disturbance waves, playing a major role in the energy transfer process from the gas to the liquid at the wall.

It is obvious from the results reported here that the use of the turbulent velocity profile, for single phase flow, in the case of relatively thin liquid films in gas/liquid pipe flow is inappropriate. However, additional accurate data will be required before concrete recommendations can be made on how to represent the velocity distribution in this case.

Acknowledgements-- Financial support by the Commission of European Communities (Contract No. JOUG-0005-C) and the General Secretariat for Research & Technology of Greece is gratefully acknowledged.

The authors also wish to acknowledge Dr. N. Andritsos, Mr. G. Georgiades and Mr. A. Lekkas for their contribution to this work.

5. REFERENCES

ADAMS, E.W., EATON, J. K. & JOHNSTON, J. P. 1984 An examination of velocity bias in a highly turbulent separated and reattaching flow. *2nd International Symposium of Application of Laser Anemometry to Fluid Mechanics* 4.1, Lisbon.

ANDRITSOS, N. 1986 Effect of pipe diameter and liquid viscosity on horizontal stratified flow. Ph.D. Thesis, University of Illinois, Urbana.

ANDRITSOS, N. & HANRATTY, T.J. 1987 Influence of interfacial waves in stratified gas-liquid flows *AIChE Jl.* **33**, 444-454.

BUCHHAVE, P., GEORGE, W.K. JR. & LUMLEY, J.L. 1979 The measurement of turbulence with the LDA. *Ann.Rev. Fluid Mech.* 11, 443-503.

CLARK, J., PALMER, M. & LAWRENCE, P. 1985 A transformation method for the reconstruction of functions from nonuniformly spaced samples. *Trans. Acous., Speech, Signal Proc.* ASSP-33(4), 1151-1165.

DRAIN, L.E. 1986 The Laser Doppler technique. J.Wiley & Sons Ltd.

FABRE, J., MASBERNAT, L. & SUZANNE, C. 1983 New results on the structure of stratified flow. *Proc. of 3rd Multiphase Flow and Heat Transfer Conference.* 1, 135-154, Miami Beach, Florida.

FUKANO, T. & OUSAKA, A. 1989 Prediction of the circumferential distribution of film thickness in horizontal and near-horizontal gas-liquid annular flows. *Int. J. Multiphase Flow* 15, 403-420.

HEWITT, G.F., JAYANTI, S, HOPE, C.B. 1990 Structure of thin liquid films in gas-liquid horizontal flow. *AERE R. 13643*, UKAEA, Harwell.

JAYANTI, S. & HEWITT, G.F. 1990 Structure of Interfacial Waves in Air-Water Horizontal Annular Flow. Presented at *ICHMT Seminar on Phase-Interface Phenomena in Multiphase Flow.* May 14-18, Dubrovnik.

KREPLIN, H.P. & ECKELMANN, H. 1979 Behavior of the three fluctuation velocity components in the wall region of a turbulent channel flow. *Phys. Fluids*, **22** (7), July.

LAURINAT, J.E., 1982 Studies of the effects of pipe size on horizontal annular two-phase flows. Ph.D. Thesis, University of Illinois, Urbana.

LAURINAT, J.E., HANRATTY, T.J. & JEPSON W.P. 1985 Film thickness distribution for gas-liquid annular flow in a horizontal pipe, *Physico Chemical Hydrodynamics*, **6** (1/2) 179-195.

McLAUGHLIN, D.K. & TIEDERMAN, W.G. 1973 Bias correction for individual realization of LDA measurements in turbulent flows. *Phys. of Fluids*, 16, 2082.

PARAS, S.V. & KARABELAS, A.J. 1991 Properties of the liquid layer in horizontal annular flow. To appear in *Int. J. Multiphase Flow*

ROSS, M. M. 1984 A LDA system for extended throw, close-to-the-wall operation in water tunnels. *2nd International Symposium of Application of Laser Anemometry to Fluid Mechanics* 10.1, Lisbon.

SAKELLARIS, B., PARAS, S.V. & KARABELAS, A.J. 1989 Data acquisition and analysis for a Laser Doppler Anemometer. *Proc. of 7th hellenic conference of application of Laser,* Athens (in Greek).

SCHLICHTING, H. 1960 Boundary layer theory, 4th edition, McGraw-Hill, New York.

SHOHAM, O. & TAITEL, Y. 1984 Stratified turbulent-turbulent gas-liquid flow in horizontal and inclined pipes. *AIChE Jl.* **30**, 377-385.

STRUMOLO, G. S., ZIEHL, W. & DUKLER, A.E. 1985 Measurements of a vertical falling film using Laser Doppler velocimetry. *2nd International Conference on Multi-phase flow,* paper G3, London, England.

VEYNANTE, D. & CANDEL, S.M. 1988 Application of nonlinear spectral analysis and signal reconstruction to LDV. *Experiments in Fluids*, 6(8),

UEDA, H. & HINZE, J.O. 1975 Fine-structure in the wall region of a turbulent boundary layer. *J.Fluid Mech.* 67 (1),125-143.

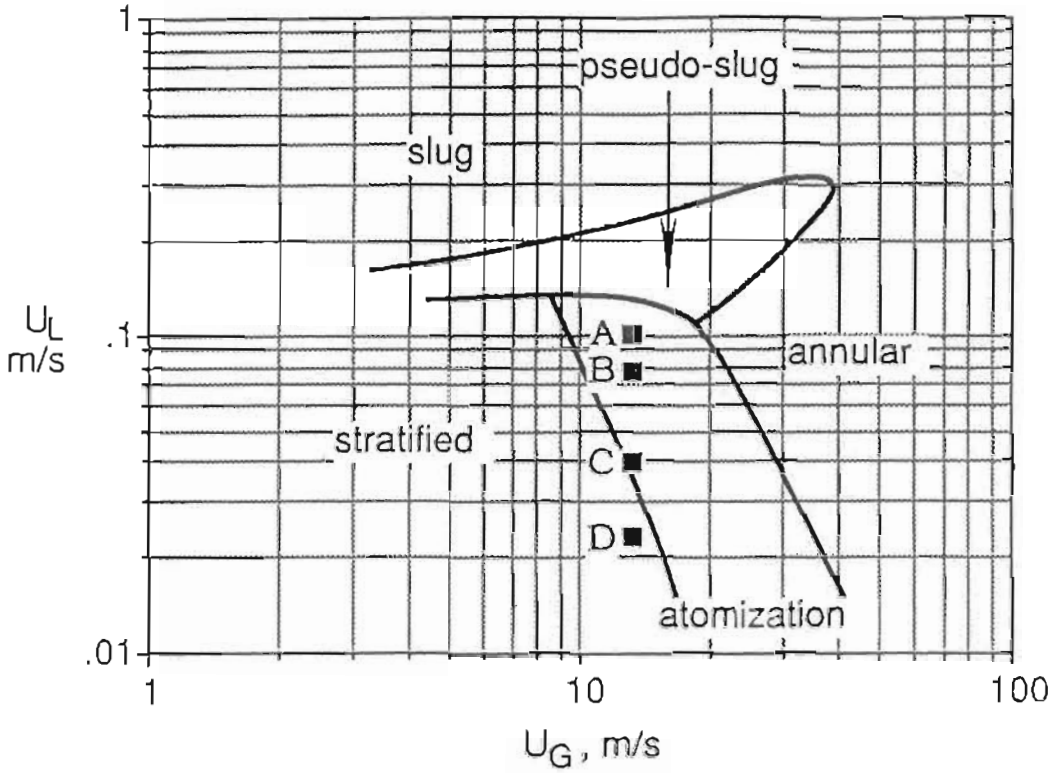

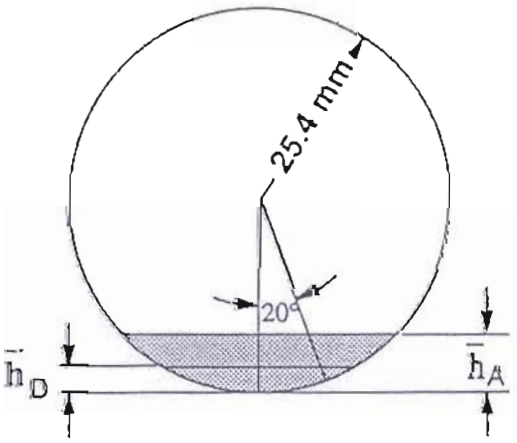

FIG. 1 FLOW REGIMES, DOMAIN OF EXPERIMENTS AND SCHEMATIC OF THE PIPE CROSS SECTION.

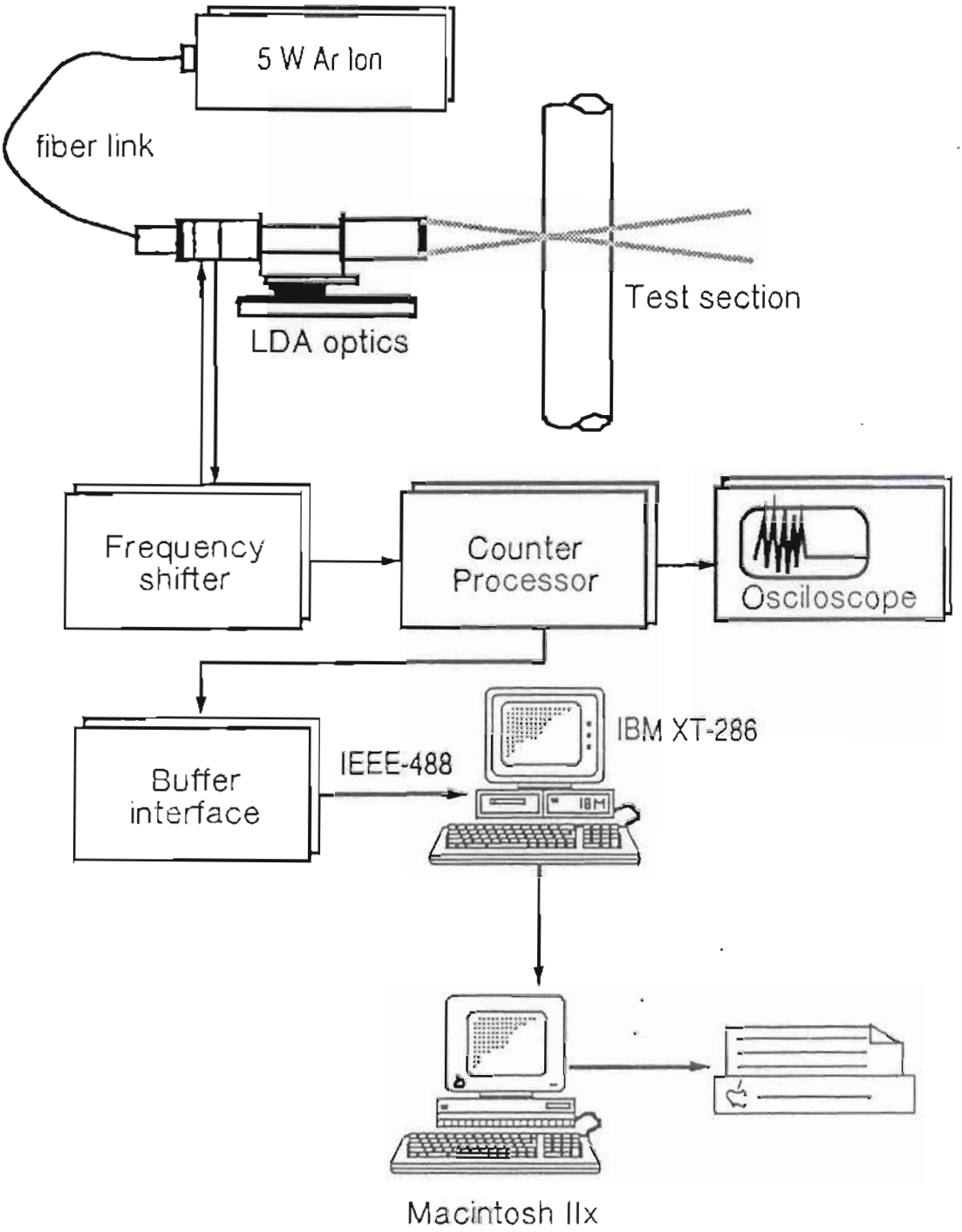

FIG. 2 GENERAL ARRANGEMENT OF THE LDA SYSTEM.

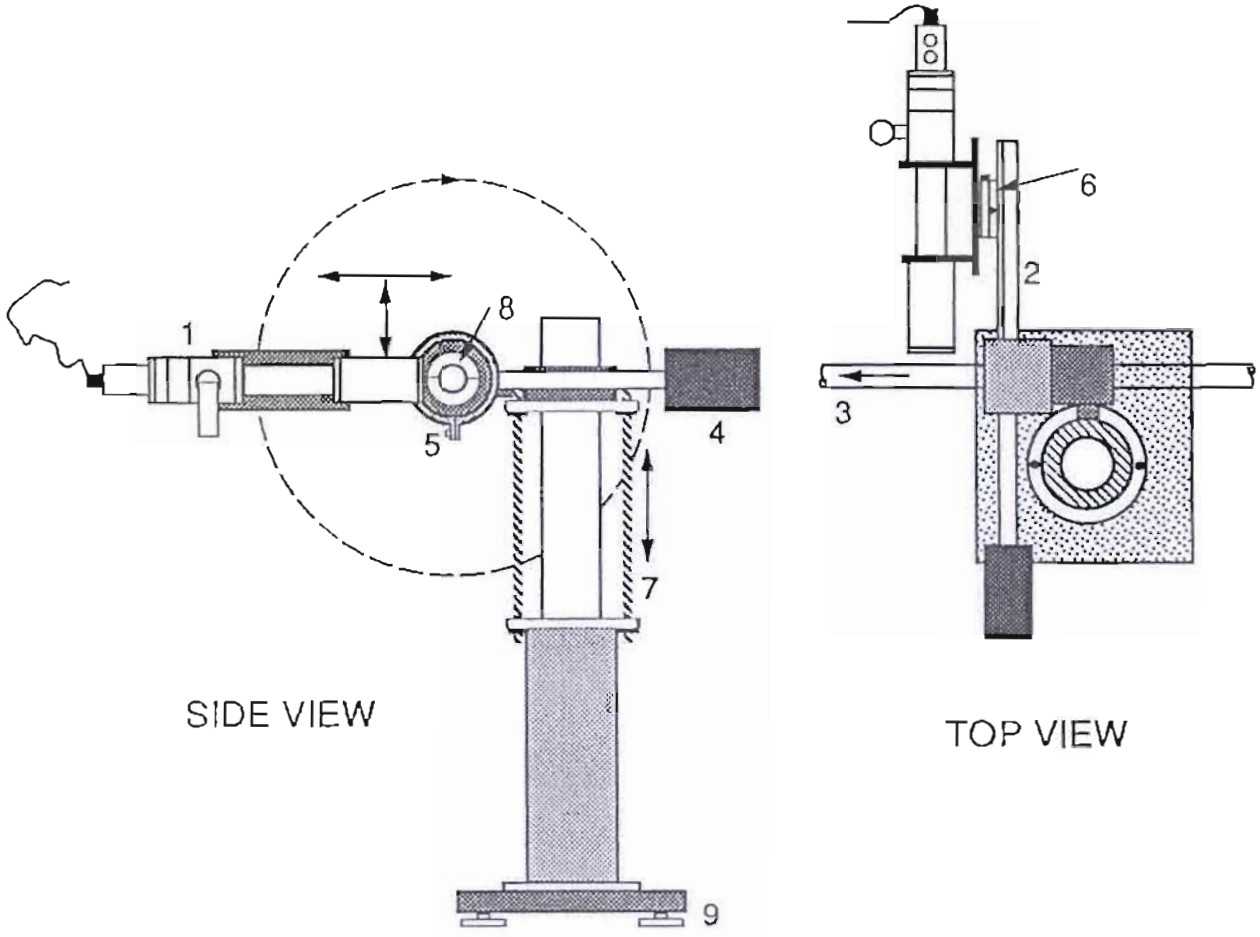

FIG. 3 SPECIAL SUPPORT UNIT FOR THE LDA OPTICS.

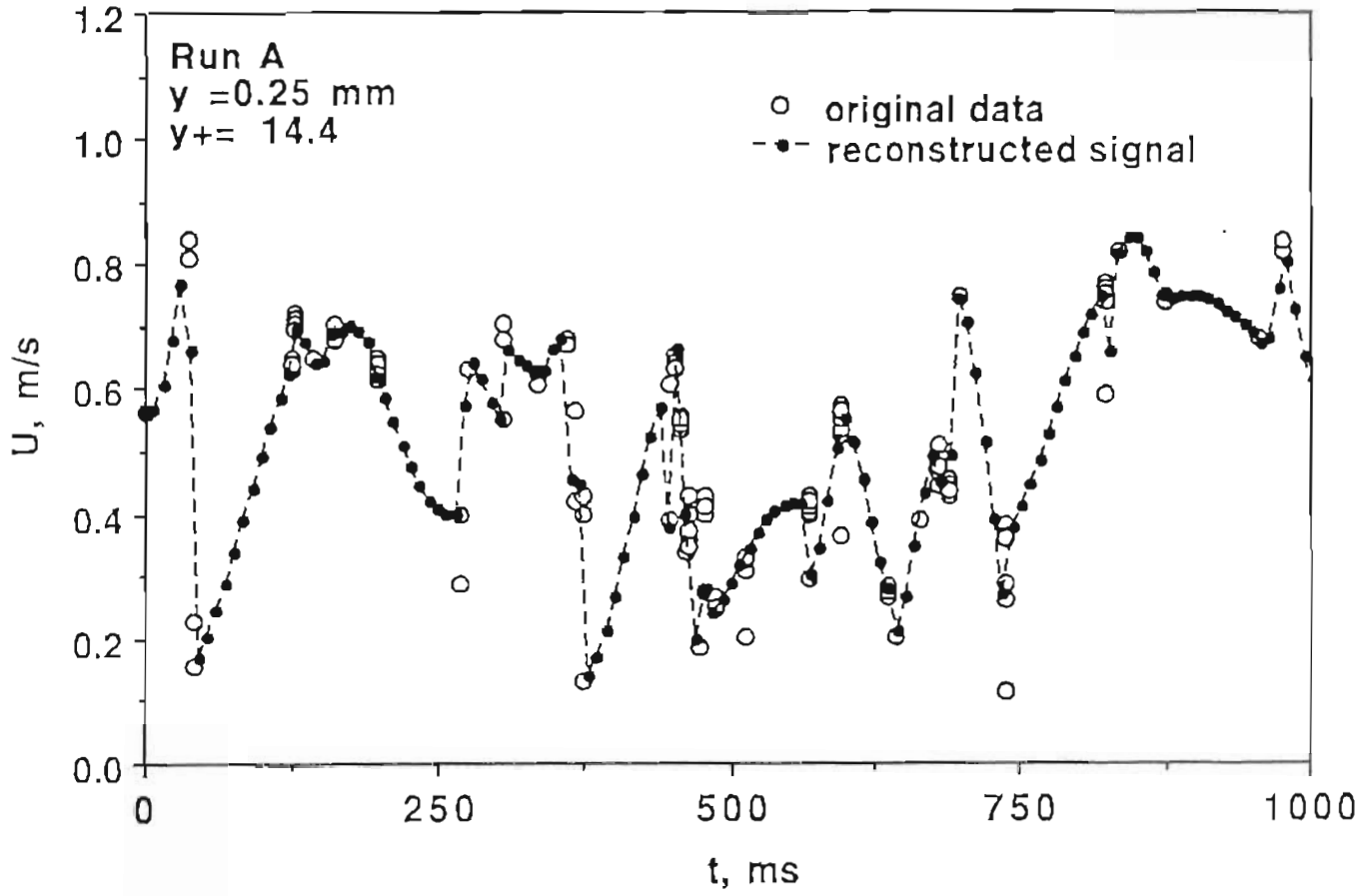

FIG. 4 TYPICAL SIGNAL OF THE AXIAL VELOCITY BEFORE & AFTER THE RECONSTRUCTION (Θ=0°)

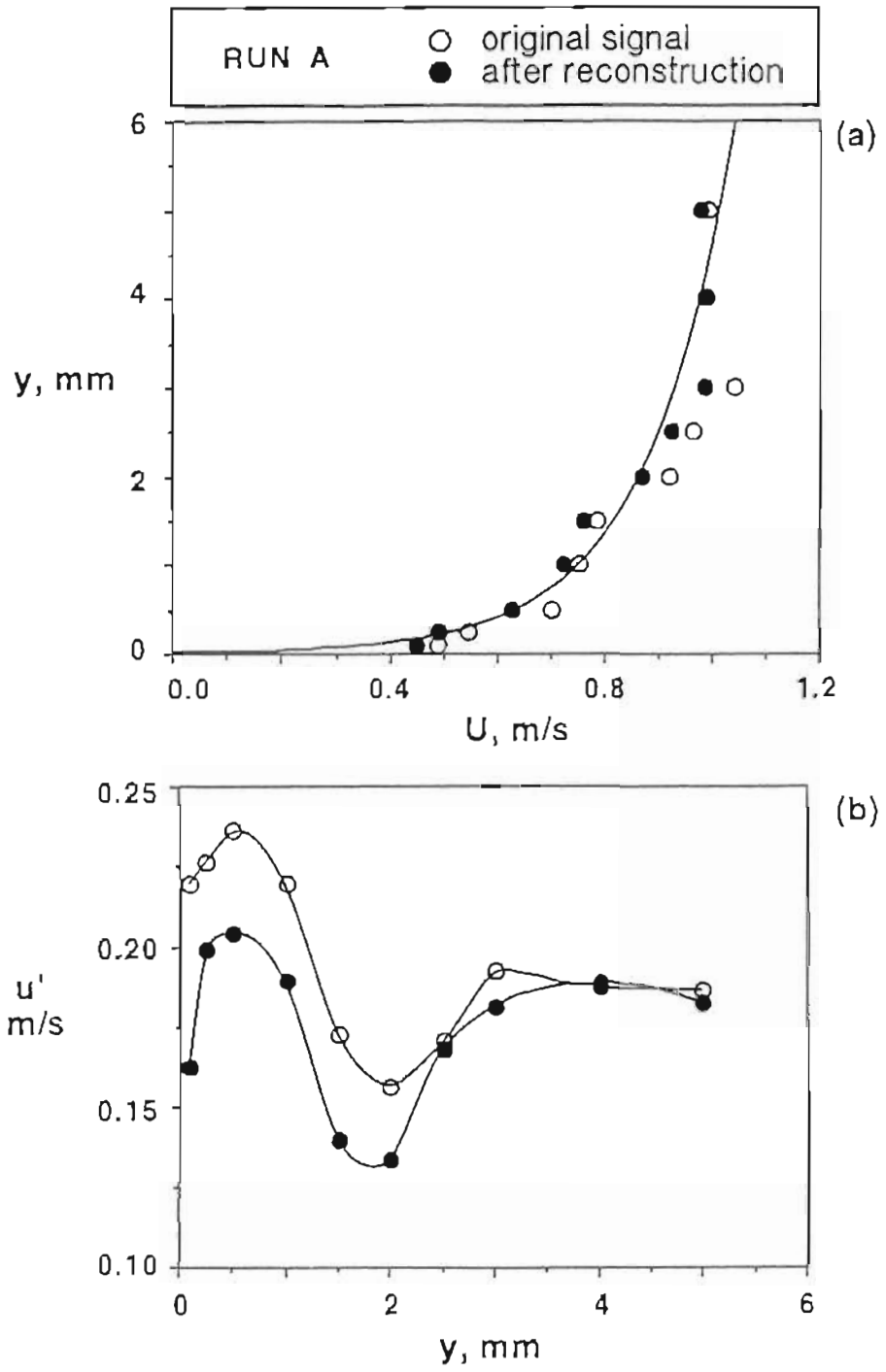

FIG. 5 a) DISTRIBUTION OF THE MEAN AXIAL VELOCITY
b) DISTRIBUTION OF THE AXIAL VELOCITY FLUCTUATIONS, BEFORE AND AFTER THE RECONSTRUCTION PROCESS (RUN A, Θ=0°).

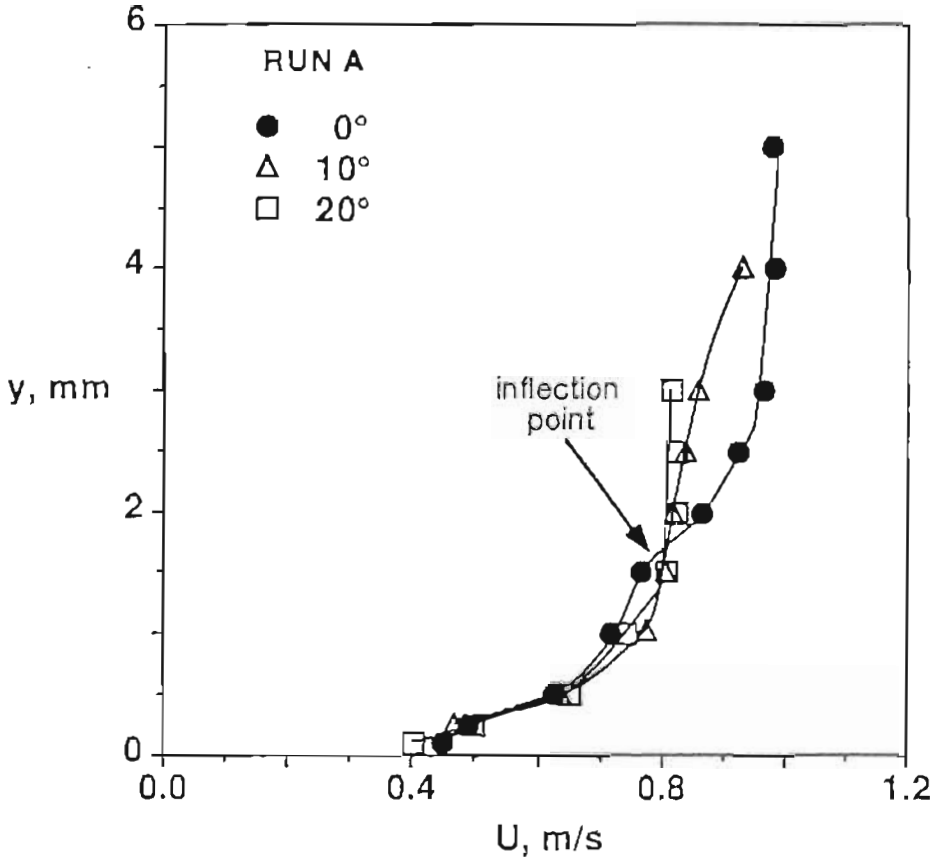

FIG. 6 AXIAL VELOCITY DISTRIBUTION FOR THREE DIFFERENT CIRCUMFERENTIAL POSITIONS (Θ=0°,10° AND 20°; RUN A)

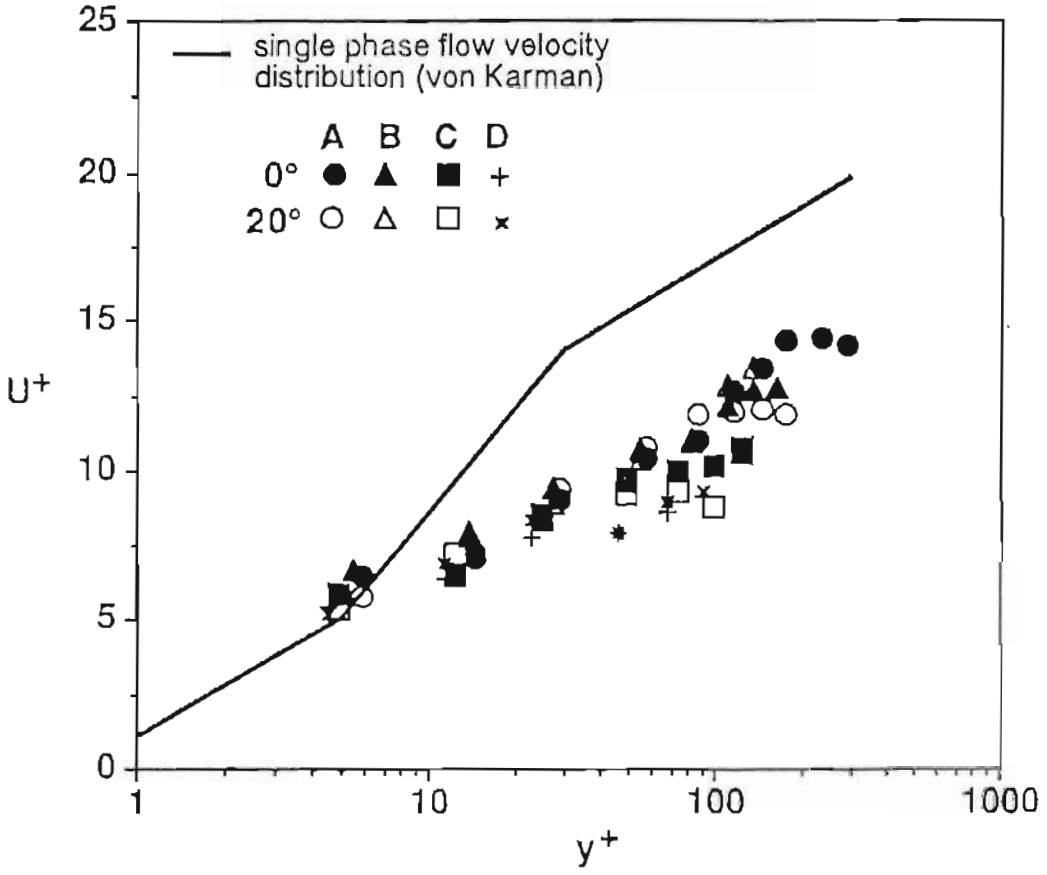

FIG. 7 DISTRIBUTION OF THE NORMALIZED TIME-AVERAGED AXIAL VELOCITY FOR ALL EXPERIMENTS (Θ=0° AND 20°)

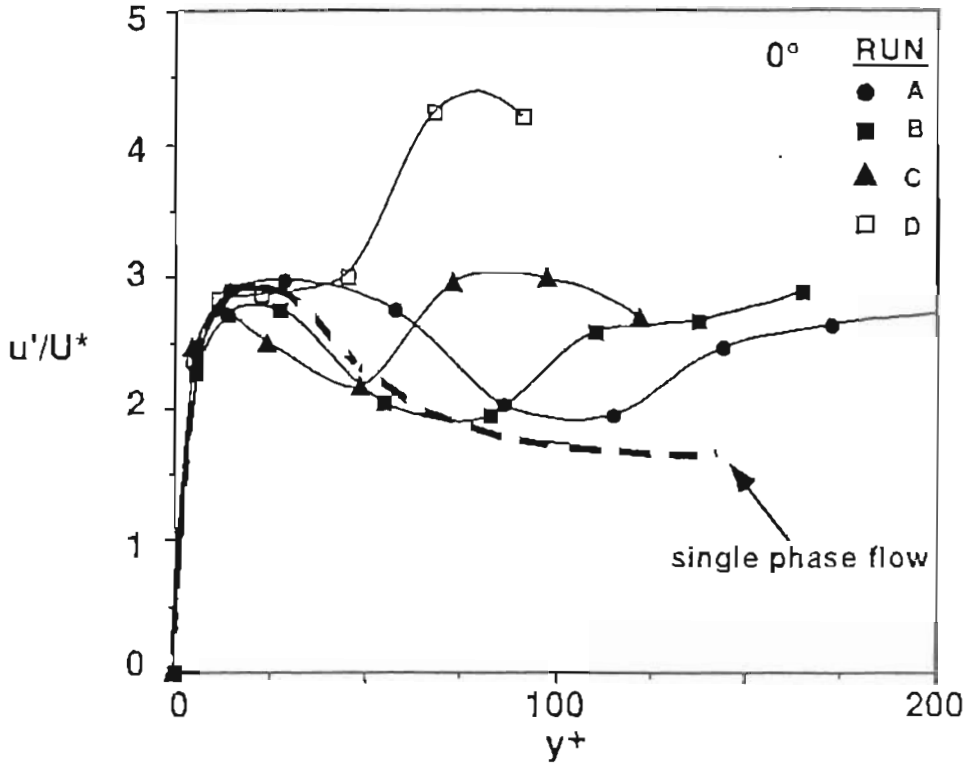

FIG. 8 DISTRIBUTION OF TURBULENCE INTENSITY AT Θ=0° FOR ALL EXPERIMENTS.

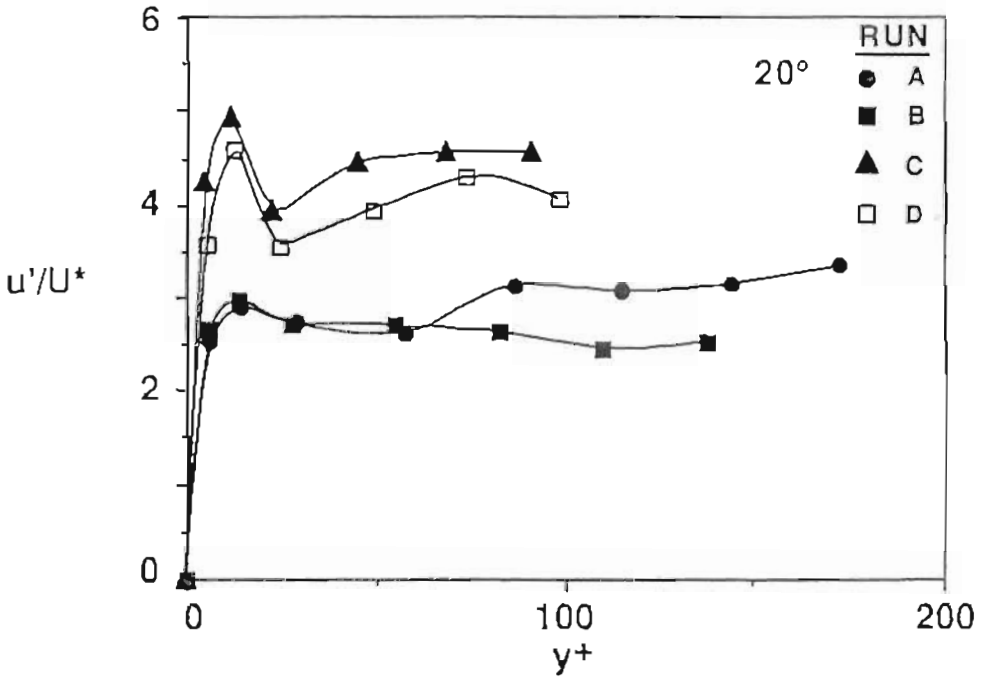

FIG. 9 DISTRIBUTION OF TURBULENCE INTENSITY AT Θ=20° FOR ALL EXPERIMENTS

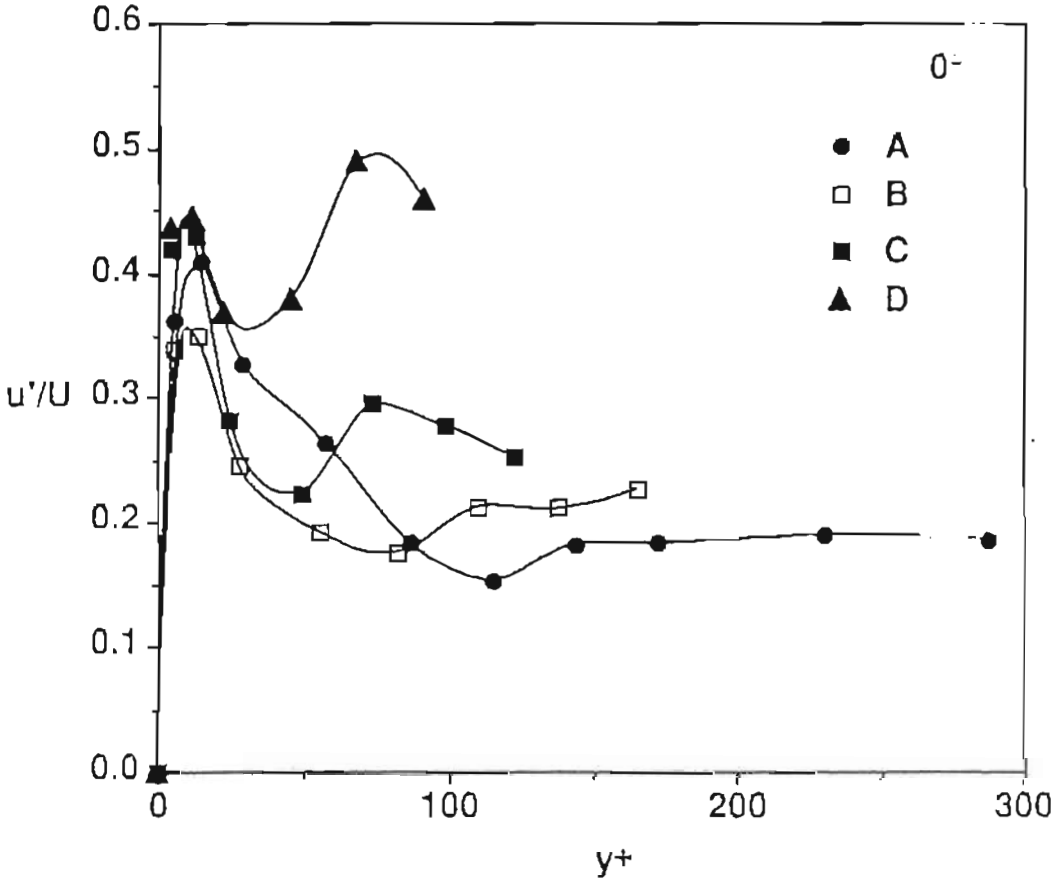

FIG. 10 DISTRIBUTION OF THE RATIO u'/U AT Θ=0° FOR ALL EXPERIMENTS

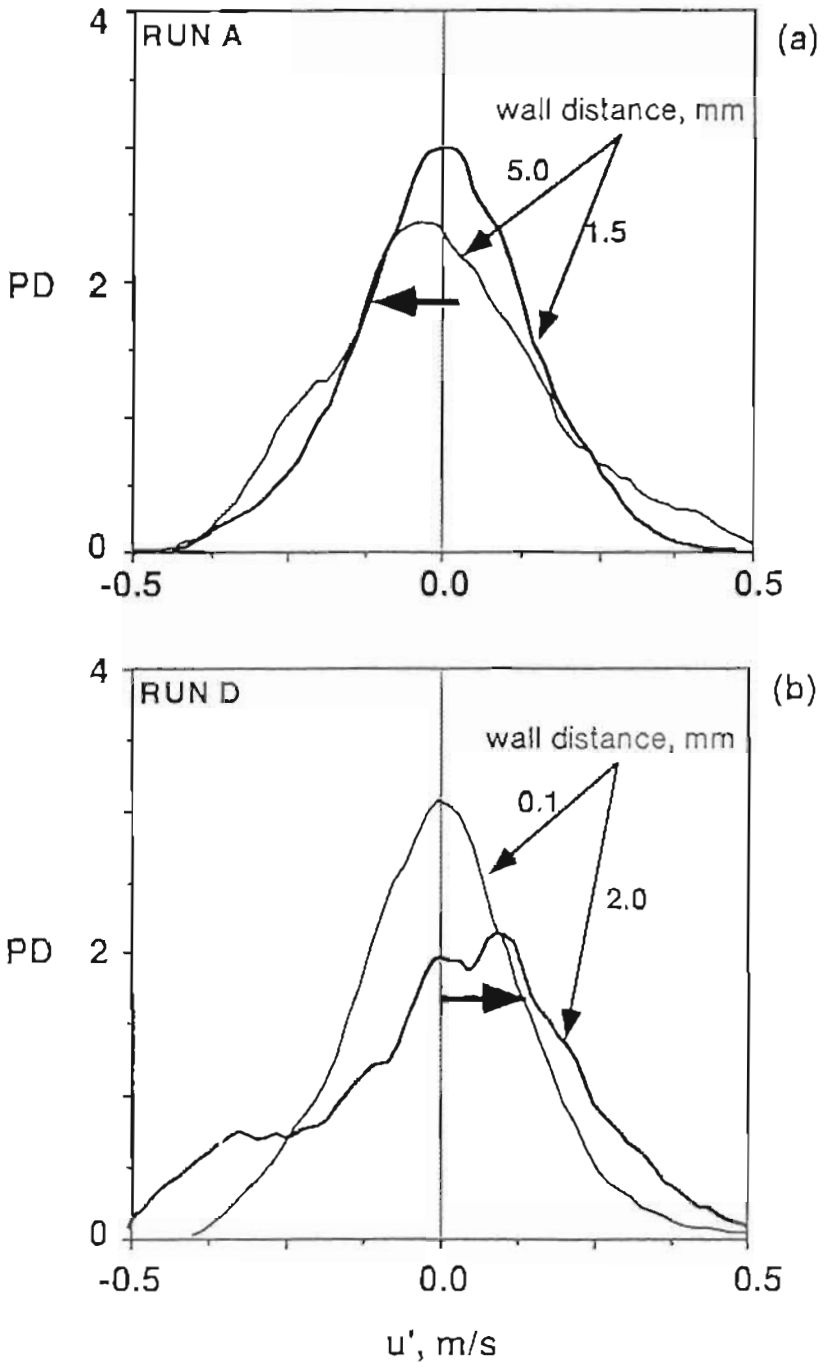

FIG. 11 PROBABILITY DISTRIBUTION OF THE AXIAL VELOCITY FLUCTUATIONS AT VARIOUS WALL DISTANCES:
a) RUN A, Θ=0°; b) RUN D, Θ=0°

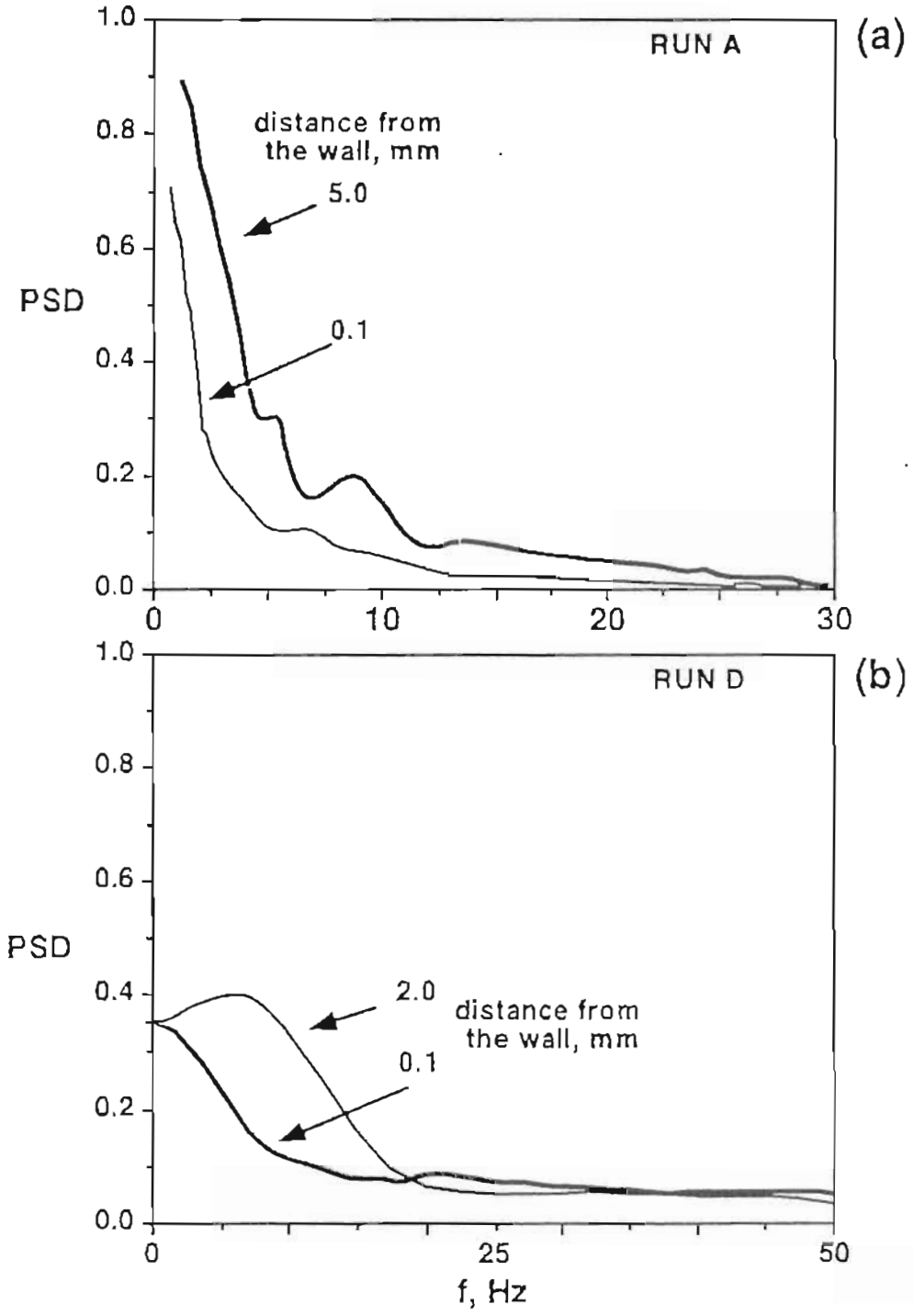

FIG. 12 POWER SPECTRAL DENSITY OF THE AXIAL VELOCITY FLUCTUATIONS AT VARIOUS WALL DISTANCES
a) RUN A, Θ=0°; b) RUN D, Θ=0°

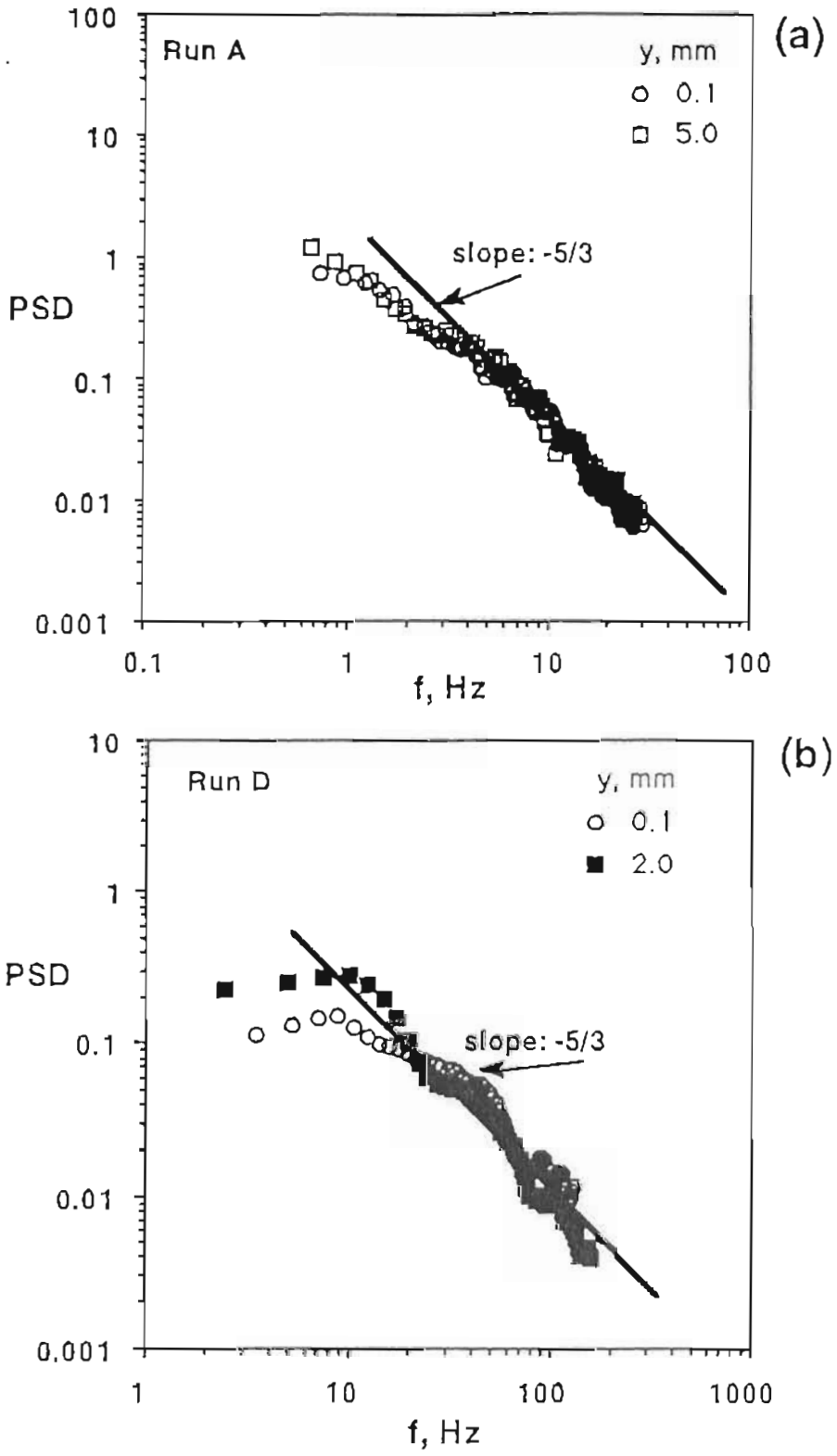

FIG. 13 POWER SPECTRAL DENSITY OF THE AXIAL VELOCITY FLUCTUATIONS AT VARIOUS WALL DISTANCES
a) RUN A, Θ=0°; b) RUN D, Θ=0°